

A Unified Dynamical Field Theory of Learning, Inference, and Emergence

Byung Gyu Chae

*Electronics and Telecommunications Research Institute,
218 Gajeong-ro, Yuseong-gu,
Daejeon 34129, Republic of Korea
bgchae@etri.re.kr*

Learning, inference, and emergence in biological and artificial systems are often studied within disparate theoretical frameworks, ranging from energy-based models to recurrent and attention-based architectures. Here we develop a unified dynamical field theory in which learning and inference are governed by a minimal stochastic dynamical equation admitting a Martin–Siggia–Rose–Janssen–de Dominicis formulation. Within this framework, inference corresponds to saddle-point trajectories of the associated action, while fluctuation-induced loop corrections render collective modes dynamically emergent and generate nontrivial dynamical time scales. A central result of this work is that cognitive function is controlled not by microscopic units or precise activity patterns, but by the collective organization of dynamical time scales. We introduce the *time-scale density of states* (TDOS) as a compact diagnostic of the distribution of collective relaxation modes governing inference dynamics. Learning and homeostatic regulation are naturally interpreted as processes that reshape both the effective potential and the underlying state-space geometry, thereby reorganizing the TDOS and selectively stabilizing slow collective modes that support stable inference, memory, and context-dependent computation despite stochasticity and structural irregularity. This framework unifies energy-based models, recurrent neural networks, transformer architectures, and biologically motivated homeostatic dynamics within a single physical description, and provides a principled route toward understanding cognition as an emergent dynamical phenomenon.

I. INTRODUCTION

Understanding how learning, inference, and stable cognition emerge from neural dynamics remains a central challenge in neuroscience and artificial intelligence [1–3]. Biological brains exhibit robust intelligent behavior despite operating with noisy, heterogeneous, and partially chaotic components [4–7], while modern artificial systems achieve impressive performance through highly engineered architectures whose organizing principles are not yet fully understood [8–11]. Unifying theories explaining why such diverse systems can support reliable inference and adaptive behavior are still lacking.

Existing approaches to neural computation typically address only limited aspects of this problem. Energy-based models, such as Hopfield networks [12, 13], provide a clear interpretation of memory as attractor dynamics but lack mechanisms for recursive reentry and temporal context integration. Biophysically detailed neuron models successfully reproduce microscopic spiking dynamics [4, 14, 15], yet offer limited insight into how large-scale collective computation and stability arise. Contemporary deep learning architectures, including transformers [9–11], demonstrate remarkable empirical success, but rely on architectural heuristics—such as residual connections, normalization, and attention—whose theoretical roles are only partially understood [16–19]. Across these paradigms, learning, inference, and emergent collective behavior are rarely treated within a single principled framework.

A closely related difficulty has long been recognized in nonequilibrium statistical physics. Macroscopic order,

collective excitations, and critical phenomena cannot be deduced directly from microscopic equations of motion [20–22]. Instead, they arise from fluctuation-dressed dynamics near soft modes and require effective descriptions formulated at the collective level. Stochastic Langevin dynamics provides a standard starting point for describing non-equilibrium systems with noise. Field-theoretic and coarse-grained approaches based on stochastic path integrals then offer a natural language for capturing such emergent behavior, separating average dynamics from fluctuation-induced effects [23–26].

Motivated by this analogy, we propose that cognition should be understood not as an explicit algorithmic computation, but as a collective dynamical phenomenon governed by an effective field-theoretic description of state-space dynamics. In this view, learning reshapes the dynamical landscape, inference corresponds to stable trajectories within that landscape, and emergent cognitive phenomena arise from the interplay between deterministic flow and stochastic fluctuations [27, 28].

In this work, we introduce a unified dynamical field theory that describes learning, inference, and emergence within a single stochastic framework. Our starting point is a minimal dynamical equation for high-dimensional collective neural states, incorporating an effective potential shaped by learning, a state-dependent geometric structure that governs sensitivity and stability, and non-conservative reentrant dynamics [29]. This formulation explicitly allows for recursive feedback and self-referential flows, which we argue are essential for stable inference and metacognitive behavior. We elevate this dynamical description to a Martin–Siggia–Rose–Janssen–de Do-

minicis (MSRJD) path-integral representation, enabling a systematic treatment of both average dynamics and fluctuations.

Within this framework, we show that inference naturally emerges as the saddle-point dynamics of the action, corresponding to the most probable trajectories of the system. Crucially, emergent collective phenomena—including critical slowing down, self-organized stability, and long-lived modes—arise inevitably from loop corrections around these saddle points [20, 30, 31]. Rather than destabilizing cognition, stochastic fluctuations play a constructive role by dynamically generating characteristic time scales and regulating collective behavior [32–34].

A central contribution of this work is to demonstrate that a wide class of existing models arise as special limits of the same underlying dynamical principle. By imposing different constraints on the effective potential, geometry, and reentrant flow, we recover Hopfield networks [12, 13], recurrent neural networks [8, 35–37], transformer architectures [9, 10], and biologically motivated homeostatic reentrant networks [38–40] as distinct realizations of the unified theory. From this perspective, the apparent diversity of learning systems reflects not fundamentally different computational mechanisms, but alternative implementations of a common dynamical structure.

Importantly, the framework advanced here entails a shift in what constitutes the fundamental object of inference. Rather than attributing cognitive function to individual neurons, synapses, or static activity patterns, we argue that inference is governed by collective dynamical modes distinguished by their characteristic time scales. In high-dimensional recurrent systems, spatial organization is largely fixed, while learning and adaptation act primarily by reshaping the temporal relaxation structure of the dynamics. We formalize this idea by introducing a *time-scale density of states* (TDOS), which quantifies the distribution of collective modes as a function of their relaxation rates. Learning reorganizes this distribution through the joint modulation of dynamical stability and state-space geometry, selectively generating slow collective modes that support stable inference, memory, and context-dependent computation despite microscopic stochasticity, random connectivity, and structural irregularity.

The remainder of this paper is organized as follows. Section II introduces the unified dynamical equation governing collective neural states, and presents the corresponding MSRJD field-theoretic formulation. In Section III, we show that inference emerges as saddle-point dynamics, while Section IV demonstrates how loop corrections generate emergent collective modes and time scales. Section V describes learning as structural adaptation, and Section VI derives several canonical learning architectures as special limits of the theory. Finally, Section VII discusses the broader implications of this framework

for neuroscience and artificial intelligence and outlines directions for future research.

II. UNIFIED DYNAMICAL DESCRIPTION OF LEARNING AND INFERENCE

A. Collective State and Unified Stochastic Dynamics

We consider a high-dimensional collective state

$$x(t) \in \mathbb{R}^N,$$

representing macroscopic neural activity in biological networks or latent representations in artificial systems. The state variable x is treated as a dimensionless coordinate in a high-dimensional state space, capturing collective degrees of freedom rather than individual microscopic units.

We propose that learning, inference, and emergent behavior are governed by the following minimal stochastic dynamical equation:

$$\dot{x}(t) = -G^{-1}(x) \nabla_x \Phi(x) + R(x) + \xi(t), \quad (1)$$

where $\Phi(x)$ is an effective potential shaped by learning, $G(x)$ is a state-dependent metric encoding the effective geometry of the collective state space, $R(x)$ is a non-conservative reentrant flow, and $\xi(t)$ denotes Gaussian white noise with variance

$$\langle \xi_i(t) \xi_j(t') \rangle = 2D \delta_{ij} \delta(t - t'). \quad (2)$$

Equation (1) constitutes a dynamical law for cognitive systems in the sense that it provides a minimal and closed description of collective dynamics. Rather than being introduced heuristically, this equation follows the standard lineage from stochastic Langevin dynamics to variational path-probability formulations. Within this framework, inference corresponds to relaxation along stable directions of the learned potential $\Phi(x)$, while the reentrant flow $R(x)$ enables iterative reinterpretation of internal states beyond simple attractor dynamics. Figure 1 schematically illustrates the conceptual structure of the unified dynamical field theory.

B. Path-Integral Formulation and Emergent Collective Modes

Equation (1) admits a MSRJD path-integral representation. Introducing response fields $\tilde{x}(t)$, the generating functional is given by

$$Z = \int \mathcal{D}x \mathcal{D}\tilde{x} e^{-S[x, \tilde{x}]}, \quad (3)$$

with the action

$$S[x, \tilde{x}] = \int dt \left[\tilde{x} \cdot (\dot{x} + G^{-1} \nabla_x \Phi - R) - D \tilde{x}^2 \right]. \quad (4)$$

This formulation provides a unified description of both average inference trajectories, corresponding to saddle points of the action, and fluctuation-induced phenomena captured by loop corrections. In particular, critical slowing down and emergent collective modes arise naturally from infrared divergences of loop diagrams near soft directions of the Hessian $\nabla^2\Phi$. The MSRJD formalism thus establishes a direct link between stochastic dynamics, inference, and emergence within a single theoretical framework.

C. Geometric Origin of the Unified Dynamical Equation

Beyond its stochastic and variational motivation, the unified dynamical equation admits a direct geometric interpretation when formulated on a Riemannian state space. We begin by viewing the collective state $x \in \mathbb{R}^N$ as a coordinate chart on a differentiable manifold endowed with a generally non-Euclidean metric $G(x)$. When the metric is state dependent, the induced geometry is intrinsically Riemannian, even though the coordinates themselves take values in \mathbb{R}^N .

On a Riemannian manifold, the most general form of a gradient flow generated by a scalar potential $\Phi(x)$ is given by

$$\dot{x}^i = -G^{ij}(x) \partial_j \Phi(x), \quad (5)$$

where $G^{ij}(x)$ denotes the inverse metric. Equation (5) represents the canonical notion of steepest descent with respect to the geometry defined by $G(x)$, and reduces to ordinary Euclidean gradient descent only when the metric is flat and constant.

However, a general vector field on a Riemannian manifold is not exhausted by gradient flows alone. Given a specified metric, any sufficiently regular drift field admits a natural decomposition into a metric-dependent gradient component and an independent, non-conservative component that is orthogonal, with respect to the inner product induced by $G(x)$, to all metric gradient vector fields. Allowing for this geometrically unavoidable remainder leads to the deterministic dynamics

$$\dot{x}^i = -G^{ij}(x) \partial_j \Phi(x) + R^i(x), \quad (6)$$

where $R(x)$ denotes a solenoidal flow that cannot be expressed as the gradient of any scalar functional.

This decomposition is closely related to Helmholtz–Hodge–type decompositions of vector fields, suitably generalized to curved (Riemannian) state spaces under standard regularity conditions [41]. Within this interpretation, the potential $\Phi(x)$ selects preferred directions of relaxation, the metric $G(x)$ determines how sensitivity is distributed across the state space, and the solenoidal term $R(x)$ captures autonomous circulation along dynamically stabilized manifolds.

This decomposition highlights a qualitative distinction between gradient-driven relaxation and reentrant dynamics. The gradient term implements inference as relaxation toward stable manifolds shaped by learning, whereas the non-conservative flow $R(x)$ redistributes activity along these manifolds without altering the value of the effective potential. Such circulation enables iterative reinterpretation, contextual modulation, and temporal looping of internal representations, extending beyond simple attractor dynamics.

Incorporating a geometrically consistent reentrant flow $R(x)$ constitutes a principled completion of the dynamical structure suggested by the underlying geometry. The unified dynamical equation thus represents the most general geometrically consistent form of a *cognitive field* on a Riemannian state space, providing a closed description that simultaneously accommodates learning-shaped potentials, adaptive state-space geometry, and non-conservative reentrant dynamics.

III. SADDLE-POINT DYNAMICS AS INFERENCE

Within the MSRJD formulation, inference corresponds to the most probable trajectory of the collective state conditioned on internal dynamics and stochastic fluctuations. This trajectory is obtained as the saddle point of the action $S[x, \tilde{x}]$, providing a dynamical realization of inference without invoking an explicit optimization algorithm.

A. Saddle-Point Dynamics and Deterministic Inference

Varying the action in Eq. (4) with respect to the response field $\tilde{x}(t)$ yields the saddle-point condition

$$\frac{\delta S}{\delta \tilde{x}(t)} = 0 \Rightarrow \dot{x}(t) = -G^{-1}(x) \nabla_x \Phi(x) + R(x), \quad (7)$$

which coincides with the deterministic component of the original Langevin dynamics in Eq. (1).

Equation (7) defines the mean inference trajectory of the system, representing the most probable evolution of the collective state in the weak-noise or large- N limit. Inference is not formulated here as an explicit minimization or symbolic computation. Instead, it emerges as a relaxation flow on a learned dynamical landscape shaped jointly by the effective potential $\Phi(x)$, the state-space geometry encoded in $G(x)$, and reentrant dynamics $R(x)$, as illustrated in Fig. 1(b).

The MSRJD path integral assigns a probability weight to each trajectory $x(t)$ according to

$$P[x(t)] \propto e^{-S[x, \tilde{x}]}. \quad (8)$$

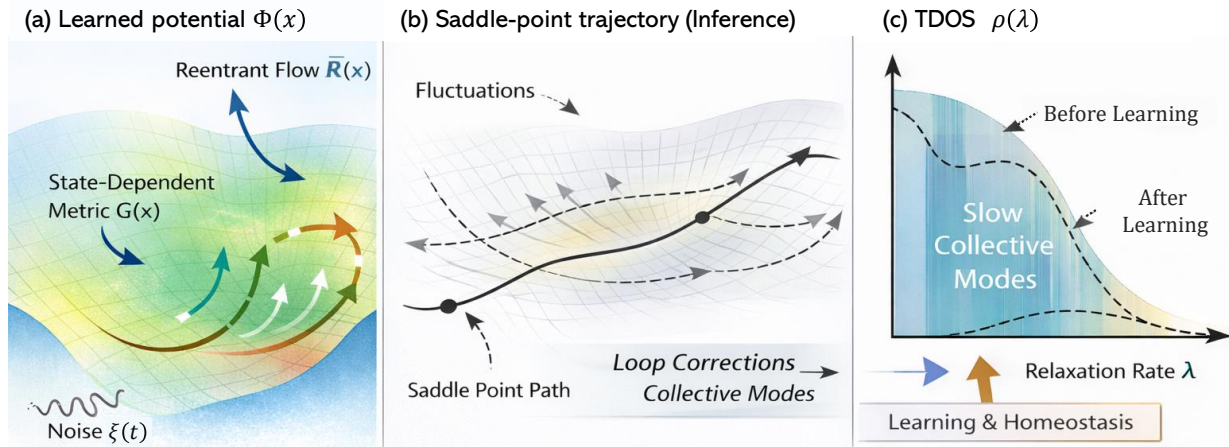


FIG. 1: Conceptual overview of the unified dynamical field theory. (a) Collective neural states evolve on a learned state-space geometry, shaped by an effective potential $\Phi(x)$, a state-dependent metric $G(x)$, non-conservative reentrant flows $R(x)$, and stochastic fluctuations $\xi(t)$. (b) Inference corresponds to saddle-point trajectories of the MSRJD action, while fluctuations around these trajectories generate emergent collective modes through loop corrections. (c) Learning and homeostatic regulation reorganize the time-scale density of states (TDOS), selectively stabilizing slow collective modes that support robust inference, memory, and context-dependent cognition.

In the small-noise limit $D \rightarrow 0$, this distribution becomes sharply peaked around the saddle-point trajectory $x^*(t)$ minimizing the effective action. Consequently, inference can be interpreted as a maximum a posteriori path selection problem,

$$x^*(t) = \arg \min_{x(t)} S_{\text{eff}}[x], \quad (9)$$

establishing an explicit equivalence between saddle-point dynamics and Bayesian inference over trajectories.

Unlike static energy-based models, the inferred object here is not a single state but an entire temporal path. Inference is therefore inherently dynamical, encoding both the evolution of internal representations and their temporal consistency. In the present framework, the saddle-point trajectory provides the deterministic backbone along which slower collective modes, generated by fluctuations, may subsequently emerge and persist.

While geometric formulations on curved state spaces have been explained in Section II, the role of state-space curvature in the present context is to regulate the sensitivity and branching of deterministic inference trajectories. Here, the metric $G(x)$ enters not as an abstract geometric object, but as an effective Fisher information metric induced by the local probabilistic sensitivity of inference dynamics [42].

When the metric $G(x)$ is non-Euclidean, nearby saddle-point inference trajectories need not remain parallel, even in the absence of noise or external perturbations. Instead, they experience relative acceleration due to the intrinsic Riemann curvature of the state space. Depending on the local sectional curvature, this geometric effect can lead to either divergence (defocusing) or convergence

(focusing) of neighboring trajectories, in direct analogy with tidal effects in general relativity.

Formally, the separation vector $\zeta^i(t)$ between two nearby inference trajectories obeys the geodesic deviation equation

$$\frac{D^2 \zeta^i}{Dt^2} = -R^i{}_{jkl}[G] \dot{x}^j \zeta^k \dot{x}^l + \dots, \quad (10)$$

where $R^i{}_{jkl}[G]$ is the Riemann curvature tensor associated with the state-space metric. We interpret this curvature-induced relative acceleration as a *cognitive tidal force*: a geometric manifestation of the information-theoretic sensitivity encoded in the Fisher metric, regulating the branching or focusing of inference trajectories independently of stochastic fluctuations (see Appendix C).

B. Observations, Reentry, and the Dynamical Nature of Inference

External observations or inputs $y(t)$ can be incorporated through an observation likelihood,

$$P[y|x] \propto \exp\left[-\frac{1}{2\sigma^2} \int dt \|Cx(t) - y(t)\|^2\right], \quad (11)$$

which adds an observation term $S_{\text{obs}}[x]$ to the action. The resulting saddle-point equation becomes

$$\dot{x}^*(t) = -G^{-1} \nabla_x \Phi(x^*) + R(x^*) - G^{-1} C^\top (Cx^* - y), \quad (12)$$

demonstrating that observations act as effective forces driving the internal state toward consistency with sensory evidence.

The reentrant term $R(x)$ plays a crucial role in this process. When $R = 0$, the dynamics reduces to pure gradient descent, leading to rapid convergence to fixed points determined solely by Φ . While sufficient for static memory retrieval, such dynamics lacks the capacity for iterative reinterpretation and contextual modulation. Beyond exploration, such reentrant flows play a crucial role in preserving tangential degrees of freedom along stabilized manifolds, thereby enabling the emergence of long-lived collective modes discussed in Sec. IV.

Taken together, Eqs. (7)–(12) imply a key conceptual shift: inference is not a discrete algorithm but a continuous dynamical relaxation along the most probable path in a learned state-space geometry. Learning shapes the potential and metric, inference follows the saddle-point dynamics of the resulting action, and cognition corresponds to stable, reentrant flows on low-dimensional manifolds.

The saddle-point description captures only the leading-order, deterministic backbone of inference. As shown in the next section, fluctuations around these trajectories generate additional collective modes and emergent time scales through loop corrections, providing a field-theoretic mechanism for emergence and criticality.

IV. LOOP CORRECTIONS AND EMERGENT COLLECTIVE DYNAMICS

The saddle-point dynamics described in Sec. III captures inference as the most probable trajectory of the system. However, saddle-point solutions alone cannot account for emergent phenomena such as critical slowing down, collective modes, or self-organized stability. These effects arise from fluctuations around inference trajectories, which are systematically captured by loop corrections in the MSRJD field theory.

A. Fluctuations Around Inference Trajectories

To analyze fluctuations, we decompose the fields as

$$x(t) = x^*(t) + \delta x(t), \quad \tilde{x}(t) = \tilde{x}^*(t) + \delta \tilde{x}(t), \quad (13)$$

where (x^*, \tilde{x}^*) satisfies the saddle-point equations. Expanding the action of Eq. (4) to quadratic order yields a Gaussian theory governing linear response and correlations, while higher-order terms generate interactions among fluctuations.

Linearizing the dynamics around the saddle point gives
$$\delta \dot{x}(t) = -M \delta x(t) + \eta(t), \quad M \equiv G^{-1} \nabla^2 \Phi|_{x^*} - \nabla R|_{x^*}, \quad (14)$$

where M is the linear stability matrix and $\eta(t)$ denotes effective noise. The corresponding retarded response function is

$$G_R(\omega) = \langle \delta x(\omega) \delta \tilde{x}(-\omega) \rangle = \frac{1}{-i\omega + M}, \quad (15)$$

and the correlation function reads

$$C(\omega) = \langle \delta x(\omega) \delta x(-\omega) \rangle = 2D G_R(\omega) G_R^\dagger(\omega). \quad (16)$$

The eigenvalues of M define a spectrum of relaxation rates governing the decay of collective perturbations. Near criticality, one or more eigenvalues approach zero, signaling the emergence of slow collective modes.

Although the reentrant flow $R(x)$ does not primarily set the dissipative relaxation rates at the Gaussian level, its gradient generically induces antisymmetric and non-normal components in the linearized stability matrix. These components generate circulation and transient amplification in state space, modifying phase structure, trajectory geometry, and sensitivity, while the dominant asymptotic relaxation rates remain controlled by the symmetric, potential-derived contribution $G^{-1} \nabla^2 \Phi$.

B. Propagators and Collective Modes in Joint State Space

Before interpreting the loop-corrected response functions, it is important to clarify the nature of the degrees of freedom being propagated. Although the unified dynamical equation is written in terms of a state vector $x(t)$, the retarded propagator G_R does not transmit states themselves. Rather, it governs the evolution of infinitesimal perturbations $\delta x(t)$ in the tangent space around an inference trajectory $x^*(t)$.

In sequence-processing systems such as recurrent networks or transformers, the state vector x naturally represents a joint configuration of multiple tokens, $x = (x_1, \dots, x_T) \in \mathbb{R}^{T \times d}$. Linearization around a saddle-point trajectory therefore defines a stability matrix M acting on the joint token state space. Its eigenvectors correspond to collective directions spanning multiple tokens and representation dimensions, while its eigenvalues set the characteristic relaxation rates of these collective modes.

The propagator of Eq. (15) thus decomposes naturally into a sum over collective eigenmodes,

$$G_R(\omega) = \sum_{\alpha} \frac{|\psi_{\alpha}\rangle \langle \tilde{\psi}_{\alpha}|}{-i\omega + \lambda_{\alpha}}, \quad (17)$$

where ψ_{α} denote collective modes in the joint state space. Apparent token-to-token influence arises from the projection of these collective modes back onto individual token coordinates. In this sense, propagation in the unified dynamical theory is mediated not by individual states, but by collective modes spanning the full state-space configuration.

More precisely, the collective modes governing fluctuation propagation are defined as eigenmodes of the linearized stability matrix M acting on the joint state space,

$$M \psi_{\alpha} = \lambda_{\alpha} \psi_{\alpha}, \quad (18)$$

where ψ_α are eigenvectors spanning coordinated directions across multiple tokens and representation dimensions, and λ_α denote the associated relaxation rates.

In this formulation, a single eigenmode ψ_α generally does not correspond to a localized perturbation of an individual token, but to a distributed collective pattern in the full token configuration space. Slow collective modes arise when one or more eigenvalues λ_α approach zero, signaling the emergence of long-lived dynamical structures.

C. Loop Corrections, Renormalization, and Time-Scale Density of States

Nonlinearities in the effective potential Φ generate interaction vertices that couple fluctuations. At one-loop order, the dominant correction to the response function is the self-energy $\Sigma_R(\omega)$, leading to the Dyson equation

$$G_R^{-1}(\omega) = G_{R0}^{-1}(\omega) - \Sigma_R(\omega). \quad (19)$$

For a generic cubic nonlinearity in the effective drift, the leading tadpole contribution yields

$$\Sigma_R^{(1)}(0) \propto \lambda \langle \delta x^2 \rangle, \quad (20)$$

where λ is an effective interaction strength. The fluctuation variance diverges as

$$\langle \delta x^2 \rangle = \int \frac{d\omega}{2\pi} C(\omega) \sim \frac{D}{\lambda_{\min}}, \quad (21)$$

with λ_{\min} denoting the smallest eigenvalue of M . As $\lambda_{\min} \rightarrow 0$, loop corrections necessarily dominate the dynamics.

To characterize the resulting structure in a manner independent of microscopic details, we introduce the *time-scale density of states*. Let $\{\lambda_\alpha\}$ denote the relaxation rates given by the real parts of the eigenvalues of M . The TDOS is defined as

$$\rho(\lambda) = \frac{1}{N} \sum_{\alpha=1}^N \delta(\lambda - \lambda_\alpha), \quad (22)$$

which may be understood in practice as a smoothed spectral density. Unlike conventional densities of states in condensed matter physics, which organize excitations by energy or momentum, the TDOS organizes collective modes purely by their temporal persistence. Figure 1(c) shows that learning and homeostatic regulation reorganize the TDOS. Physically relevant behavior does not arise from a single relaxation rate, but from the accumulation of spectral weight near slow time scales (See the details in Appendix A).

Including the one-loop correction, the renormalized relaxation rate m of the slowest mode satisfies the self-consistent relation

$$m = m_0 + c \frac{\lambda D}{m}, \quad (23)$$

where m_0 is the bare relaxation rate, D denotes the low-frequency fluctuation power (so that λD has units of m^2), and c is a numerical constant set by the loop integral and regularization scheme. At the nominal mean-field critical point $m_0 = 0$, this yields the finite solution

$$m = \sqrt{c\lambda D} \sim \sqrt{\lambda D}, \quad (24)$$

showing that fluctuations dynamically generate an effective infrared cutoff through a Dyson self-consistency. Learning and homeostatic regulation can then be interpreted as processes that reshape the temporal density of states, selectively enhancing or suppressing collective modes at specific time scales.

D. Emergent Collective Modes and Physical Interpretation

The pole structure of the renormalized response function,

$$G_R(\omega) \sim \frac{1}{-i\omega + m}, \quad (25)$$

defines a *dressed* collective relaxation mode with lifetime $\tau \sim m^{-1}$. While such slow modes exist already at the bare (mean-field) level with rate m_0 , fluctuation-induced self-energy effects renormalize and regulate it, generating a self-organized infrared scale even in the limit $m_0 \rightarrow 0$.

We interpret such regulated quasi-soft excitations as carriers of emergent computation and memory, analogous to quasiparticles in condensed-matter systems. Specifically, we define a *neuroton* as a self-generated collective relaxation mode arising from fluctuation-induced dressing around a reentrant saddle-point dynamics. Neurotons correspond to long-lived collective excitations associated with low-frequency poles of the retarded Green's function in the joint state space, representing coordinated dynamical patterns spanning multiple tokens and representation dimensions near the homeostatically stabilized shell. In this sense, they are analogous to Goldstone-like modes, representing protected angular fluctuations whose effective energy scale is set by inverse relaxation times rather than microscopic Hamiltonians.

At a more general level, the loop expansion reveals a universal mechanism for emergence: whenever nonlinear interactions and stochastic fluctuations coexist, new collective time scales are dynamically generated beyond mean-field dynamics. Within the present framework, saddle-point dynamics implements inference, loop corrections give rise to emergent collective modes such as neurotons, and critical behavior arises from the competition between deterministic drift and fluctuation-induced self-energy.

V. LEARNING AS STRUCTURAL ADAPTATION AND TDOS REORGANIZATION

The preceding sections have established the dynamical principles governing inference and emergence. Inference arises as saddle-point dynamics of the unified action, while fluctuation-induced loop corrections generate collective modes and emergent time scales. We now address how *learning* operates within this framework.

In the present theory, learning is not an independent algorithmic procedure, nor an external optimization rule imposed on the dynamics. Instead, learning is identified with a slow structural adaptation of the unified dynamical system, driven by the statistics of inference trajectories and their associated collective modes. Crucially, learning acts by reorganizing the distribution of dynamical time scales uncovered by the loop analysis, thereby shaping the temporal architecture of cognition. Equivalently, learning reshapes the spectrum of collective modes—neurotons—that can be sustained by the dynamics, thereby controlling which long-lived trajectories remain available for inference.

A. Learning as Slow Structural Adaptation

At the level of the unified dynamical equation, no explicit distinction is made between inference and learning. Both processes are governed by the same stochastic dynamics. The distinction emerges from a separation of time scales between fast state evolution and slow structural change.

We identify learning with the gradual adaptation of the structural components of the dynamics, $\theta \equiv \{\Phi(x), G(x), R(x)\}$, which evolve on a time scale much slower than the collective state $x(t)$,

$$\dot{\theta} = \epsilon \left\langle \mathcal{F}(x(t), y(t)) \right\rangle_{\text{inference}}, \quad \epsilon \ll 1, \quad (26)$$

where $\langle \cdot \rangle_{\text{inference}}$ denotes an average over inference trajectories generated under the current structure.

Equation (26) expresses the principle that learning is driven by the accumulated statistics of inference rather than by instantaneous fluctuations. Repeated inference episodes under similar inputs bias the structural parameters so as to stabilize frequently visited trajectories and destabilize inconsistent ones. From the perspective of Sec. IV, this stabilization corresponds to the selective reinforcement of slow collective modes in the joint state space, while fast-decaying modes are progressively suppressed. Learning therefore sculpts the geometry of state space, making correct inference dynamically natural rather than algorithmically enforced.

In supervised settings, external targets repeatedly constrain inference trajectories toward desired outcomes.

Structural adaptation then reshapes the effective potential and metric so that trajectories consistent with correct outputs correspond to low-action paths. In unsupervised settings, no explicit targets are provided; instead, frequently encountered input patterns induce reproducible inference trajectories, which are progressively stabilized through structural adaptation. Representation learning thus corresponds to the emergence of stable low-dimensional inference manifolds.

B. Learning as Reorganization of the Time-Scale Density of States

The loop analysis of Sec. IV revealed that fluctuations around inference trajectories are governed by a spectrum of collective modes organized by their relaxation time scales. These modes, rather than microscopic degrees of freedom, constitute the effective carriers of inference dynamics.

From this perspective, learning operates by reorganizing the *time-scale density of states* associated with collective modes. Structural adaptation selectively enhances slow collective modes associated with behaviorally relevant features of the input statistics, while suppressing fast, unstable fluctuations. Individual collective modes (neurotons) provide the dynamical carriers of computation, but meaningful information is encoded only at the level of their organized temporal spectrum, as captured by the TDOS.

Learning therefore accumulates information by reshaping the temporal spectrum of collective dynamics. Stable inference, memory, and context-dependent computation correspond to the presence of robust spectral weight at long time scales, while homeostatic regulation prevents uncontrolled critical slowing down. In this way, learning transforms the emergent collective dynamics into a stable substrate for intelligent behavior.

VI. SPECIAL LIMITS: FROM ENERGY-BASED MODELS TO REENRANT ARCHITECTURES

The unified dynamical equation introduced in Sec. II provides a common theoretical framework encompassing a wide class of learning systems. In this section, we demonstrate that several canonical models—including Hopfield networks [12, 13], recurrent neural networks (RNNs) [35, 36], transformers [9, 10], and our fast-weights homeostatic reentry network (FHRN) model [38, 39]—arise as distinct limits of the same underlying dynamics.

A. Hopfield Networks: Pure Gradient Descent Limit

We first consider the limit in which reentrant dynamics and stochastic fluctuations are absent,

$$R(x) = 0, \quad \xi(t) = 0, \quad (27)$$

and the metric reduces to the Euclidean form,

$$G = I. \quad (28)$$

If the effective potential $\Phi(x)$ is identified with an explicit energy function $E(x)$, the unified dynamical equation reduces to

$$\dot{x} = -\nabla E(x), \quad (29)$$

which is precisely the continuous-time Hopfield dynamics.

In this limit, inference corresponds to relaxation toward local minima of the energy landscape, while stored memories are represented by stable fixed points. Hopfield networks therefore realize the purely conservative limit of the unified theory, in which cognition is identified with convergence to static attractors.

From the present perspective, this limit is characterized by a fixed state-space geometry, the absence of non-conservative reentrant flows, and a restricted repertoire of dynamical time scales. As a result, while Hopfield networks provide a clear model of associative memory, they lack mechanisms for iterative reinterpretation, contextual modulation, and the emergence of rich collective dynamics.

B. Recurrent Neural Networks: Discrete-Time Approximation

We next show how standard recurrent neural networks arise as discrete-time approximations to the unified continuous dynamics. Starting from Eq. (1), a forward Euler discretization yields

$$x_{t+1} = x_t + \Delta t [-G^{-1}\nabla\Phi(x_t) + R(x_t)]. \quad (30)$$

To connect this expression to the conventional update, it is useful to isolate a baseline leak term and interpret the remaining drift as an effective recurrent interaction. In the Euclidean limit $G = I$, consider first a quadratic effective potential

$$\Phi(x) = \frac{1}{2}\|x\|^2 - \frac{1}{2}x^\top Wx - b^\top x, \quad W = W^\top, \quad (31)$$

for which

$$-\nabla\Phi(x) = -x + Wx + b. \quad (32)$$

More generally, for an arbitrary smooth drift $F(x) \equiv -G^{-1}(x)\nabla\Phi(x)$, linearization around a reference state

x_0 yields $F(x) \approx F(x_0) + J_F(x_0)(x - x_0) = Ax + b_{\text{eff}}$. Decomposing $A = -I + W$ then gives the canonical form

$$-G^{-1}\nabla\Phi(x) \approx -x + Wx + b. \quad (33)$$

Substituting this approximation into Eq. (30) and absorbing constants into a nonlinear activation function leads to

$$x_{t+1} = f(Wx_t + b), \quad (34)$$

which is precisely the standard update rule.

From the present perspective, RNNs can be viewed as discrete-time approximations of the unified continuous dynamics, in which inference is implemented as iterative relaxation under a locally linearized effective potential. The recurrence in RNNs thus provides a basic form of temporal feedback, while the discrete time step Δt imposes an externally fixed time scale.

More generally, if the effective recurrent interaction contains an antisymmetric component, the resulting discrete-time dynamics may also exhibit nonconservative circulation, corresponding to the reentrant term $R(x)$ in the continuous formulation. Such effects can give rise to non-normal dynamics and transient amplification beyond pure gradient relaxation, but they are not structurally constrained and need not be confined to stable manifolds. As a result, such circulation does not generically give rise to protected long-lived collective modes or a reorganized time-scale density of states.

Element-wise nonlinearities such as sigmoidal activation functions introduce local, state-dependent gain modulation and play an important role in stabilizing individual units. However, these nonlinearities do not induce a learned geometry of the collective state space. As a result, while RNNs can represent temporal dependencies and sequential structure, they lack intrinsic mechanisms for dynamically shaping state-space geometry or redistributing collective time scales through self-generated collective modes.

C. Transformer Architectures: Linear Attention and Discrete Recurrent Dynamics

Transformer architectures are often described as feed-forward models. However, recent work has shown that autoregressive transformers with linearized attention mechanisms can be reformulated exactly as recurrent dynamical systems with explicitly maintained state variables [19]. From the present perspective, this result clarifies the precise dynamical status of transformers within the unified framework.

For causal linear attention, the output at time step t can be written as

$$y_t = \frac{\phi(q_t)^\top \sum_{j \leq t} \phi(k_j)v_j^\top}{\phi(q_t)^\top \sum_{j \leq t} \phi(k_j)}, \quad (35)$$

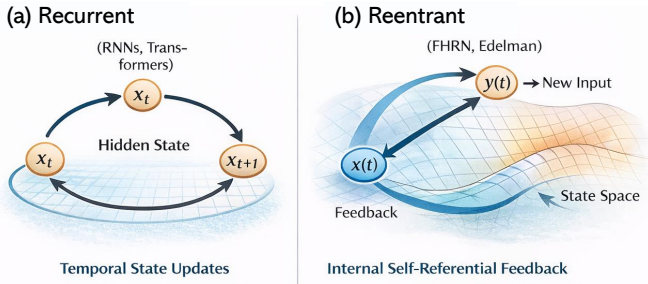


FIG. 2: Recurrent versus reentrant neural architectures. (a) Recurrent architectures update a latent hidden state sequentially in time. The recurrence operates through discrete or implicit temporal state updates, while the underlying representation space and geometry remain fixed. Temporal dependencies are captured by iterating the same state-transition rule across time steps. (b) Reentrant architectures implement internal self-referential feedback at the same representational level. Here, the system’s output is continuously fed back as a new input, dynamically reshaping the effective state-space geometry and collective dynamics. Reentry enables reflective computation, context-dependent reinterpretation, and dynamical modulation of collective modes beyond simple temporal recurrence.

where $\phi(\cdot)$ denotes a feature map. Introducing cumulative state variables

$$S_t = S_{t-1} + \phi(k_t)v_t^\top, \quad Z_t = Z_{t-1} + \phi(k_t), \quad (36)$$

the transformer update can be expressed in explicitly recurrent form,

$$(S_t, Z_t) = \mathcal{R}((S_{t-1}, Z_{t-1}), x_t), \quad (37)$$

with outputs obtained through a state-dependent normalization. Thus, autoregressive transformers with linear attention implement recurrent dynamics over *collective memory variables*, rather than over individual neuron activations.

Within the unified dynamical field theory, this recurrence corresponds to a fixed reentrant-like flow acting on an augmented state space, with the qualifier that its structure is externally specified rather than dynamically learned. The normalization by Z_t induces an implicit, architecture-prescribed scaling that may be interpreted as a constrained or fixed metric structure. Crucially, however, both the recurrence rule and the effective geometry are externally specified by the model design and do not evolve dynamically with the system state.

Residual connections commonly used in transformer blocks can be viewed as a numerically stable discretization of such recurrent updates along network depth. While this interpretation highlights the stability of information flow, it is not the fundamental source of temporal integration or memory in transformers. The essential dynamical mechanism is instead the recurrent accumulation of collective state variables through attention.

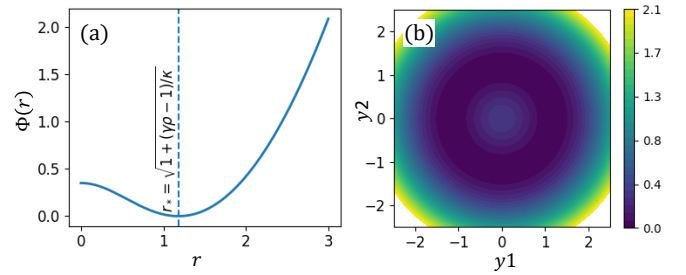


FIG. 3: Effective homeostatic potential of the Fast-weights Homeostatic Reentry Network. (a) One-dimensional radial effective potential $\Phi(r)$ obtained from the exact radial reduction of the FHRN dynamics. For $\gamma\rho > 1$, the potential develops a nontrivial minimum at a finite radius $r^* = \sqrt{1 + (\gamma\rho - 1)/\kappa}$, corresponding to a stable homeostatic shell. The origin $r = 0$ is unstable, while radial fluctuations are strongly stabilized near $r = r^*$. (b) Two-dimensional visualization of the same effective potential $\Phi(y_1, y_2) = \Phi(y_1^2 + y_2^2)$ in the full state space. The Mexican-hat-like geometry illustrates radial stabilization combined with a flat angular direction, providing a geometric substrate for collective computation. Reentrant dynamics generate non-conservative flows along the shell, while the potential enforces homeostatic control of activity magnitude.

Consequently, transformers realize a discrete-time recurrent approximation of the unified dynamical equation, enabling efficient integration of long-range dependencies through structured memory accumulation. At the same time, they lack mechanisms for state-dependent reorganization of collective mode structure or for dynamically reshaping the distribution of intrinsic time scales. As a result, long-lived collective excitations in transformers remain architecture-imposed rather than dynamically generated. In this sense, transformer architectures occupy an intermediate regime: they go beyond purely feedforward models by implementing recurrence at the level of collective memory, yet remain distinct from genuinely reentrant systems in which the effective geometry and stability structure are dynamically modulated by the system’s own activity.

D. FHRN Model: Homeostatic Reentrant Dynamics with Dynamic Geometry

We have introduced the homeostatically regulated reentry network [38, 39], which realizes the unified dynamical equation in a regime where *state-space geometry itself is dynamically generated*. Unlike standard recurrent or transformer architectures, where the effective geometry is externally imposed or fixed, the FHRN induces a state-dependent metric through homeostatic regulation. Figure 2 illustrates the conceptual distinction between recurrent and reentrant processes.

The continuous-time FHRN dynamics is defined by

$$\dot{y} = -y + \gamma W[g(r)y], \quad r = \|y\|, \quad (38)$$

where $y \in \mathbb{R}^N$ denotes collective population activity, W is a fixed mixing matrix with dominant eigenvalue ρ , γ controls reentry strength, and $g(r)$ is a homeostatic gain function.

Projecting Eq. (38) onto the dominant eigenmode of W yields an exact radial equation,

$$\dot{r} = [-1 + \gamma\rho g(r)]r, \quad (39)$$

which admits a gradient representation

$$\dot{r} = -\frac{d\Phi(r)}{dr}. \quad (40)$$

For the homeostatic gain $g(r) = [1 + \kappa(r^2 - 1)]^{-1}$, the effective potential takes the explicit form

$$\Phi(r) = \frac{1}{2}r^2 - \frac{\gamma\rho}{2\kappa} \ln[1 + \kappa(r^2 - 1)]. \quad (41)$$

Equation (41) stabilizes activity on a finite-radius shell for $\gamma\rho > 1$, strongly suppressing radial fluctuations. This stabilization can be interpreted as the emergence of an *anisotropic metric* on state space, in which radial directions are stiff while tangential directions remain soft. From an information-geometric perspective, this dynamically generated anisotropic metric admits a natural interpretation as an effective Fisher information metric induced by homeostatic suppression of radial uncertainty, as detailed in Appendix D. Figure 3 provides explicit visualizations of the effective homeostatic potential emerging from the FHRN dynamics. These figures complement the analytical derivation by illustrating how radial stabilization and angular degeneracy jointly produce a shell-shaped attractor manifold.

Within the unified dynamical equation

$$\dot{x} = -G^{-1}(x) \nabla_x \Phi(x) + R(x), \quad (42)$$

the FHRN corresponds to a geometry in which the metric takes the projected form

$$G(y) = g_r(r) P_r + g_\perp(r) P_\perp, \quad P_r = \frac{yy^\top}{r^2}, \quad P_\perp = I - P_r, \quad (43)$$

with $g_r(r) \gg g_\perp(r)$ for $\gamma\rho > 1$. Crucially, this metric is not imposed externally but is generated dynamically through homeostatic feedback (See the details in Appendix B).

The remaining tangential dynamics along the shell is governed by a non-conservative reentrant flow,

$$R(y) = \gamma g(r) P_\perp W y, \quad (44)$$

which induces collective mixing without altering the stabilized radial amplitude. This flow cannot be derived

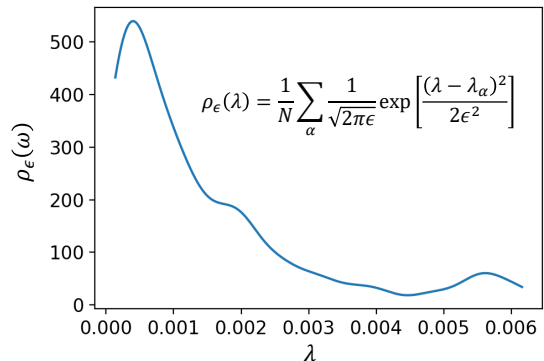


FIG. 4: Time-scale density of states $\rho_\epsilon(\lambda)$ of the FHRN. The TDOS is computed by linearizing the deterministic dynamics $\dot{x} = -\nabla\Phi(x) + R(x)$ around a stable homeostatic fixed point x^* , forming the stability matrix $M = -\partial F/\partial x|_{x^*}$, and smoothing the real parts of its eigenvalues with a Gaussian kernel.

from a scalar potential and represents a genuine form of reentry in the sense of Edelman: the system's own output is reinjected to reorganize internal dynamics [1, 2].

Figure 4 displays the TDOS of the FHRN, extracted from the spectrum of the linearized dynamics around a stable homeostatic fixed point, revealing a dense accumulation of slow collective modes. The pronounced accumulation of modes at small relaxation rates λ reveals a dense spectrum of slow collective modes generated by the interplay of homeostatic stabilization and antisymmetric reentrant mixing. These long-lived modes dominate inference dynamics and provide a dynamical substrate for memory and temporal integration. These modes correspond precisely to the neurotons introduced in Sec. IV. The continuous structure of the TDOS highlights that cognition in the FHRN is governed by the collective organization of time scales rather than by isolated modes or fixed points.

In contrast to transformer architectures, where normalization layers approximate a fixed, externally designed geometry, the reentry network dynamically reshapes its effective metric in response to activity. Homeostasis sculpts the geometry, while reentry drives computation along the resulting low-dimensional manifold.

Thus, the FHRN realizes the unified dynamical theory in a regime where learning and inference are mediated not only by an effective potential, but by the endogenous emergence of state-space geometry itself.

E. Unifying Perspective

The above limits establish a hierarchy of expressive power within the unified dynamical framework. Specifically, commonly studied architectures correspond to increasingly general realizations of the same underlying dy-

namical law,

$$\begin{aligned} \text{Hopfield} \subset \text{RNN} \subset \text{Transformer} \subset \\ \text{Unified Dynamical Field Theory}, \end{aligned} \quad (45)$$

where the inclusion relation is understood in a *dynamical* rather than architectural sense.

In this hierarchy, each class expands the set of admissible dynamical structures—effective potentials Φ , reentrant flows R , and normalization or geometric constraints—while remaining describable as a special limit of the same stochastic dynamical equation. Hopfield networks correspond to pure gradient descent in a fixed Euclidean geometry, recurrent neural networks introduce discrete-time recurrence with externally imposed temporal structure, and transformer architectures further incorporate state-dependent recurrent mixing and normalization.

The FHRN model occupies a distinct regime within this unified description. Unlike standard recurrent or attention-based architectures, the FHRN dynamics generates both an effective potential and a state-dependent, anisotropic metric endogenously through homeostatic regulation. As a result, the geometry of the collective state space and the distribution of relaxation time scales are themselves dynamical objects, rather than externally prescribed design choices.

From this perspective, the apparent diversity of learning architectures reflects not fundamentally different computational principles, but different constraints on how Φ , G , and R are realized. The unified dynamical field theory thus provides a common language in which these models can be compared, extended, and systematically generalized.

VII. DISCUSSION AND OUTLOOK

A. Inference, Geometry, and Emergence as a Unified Dynamical Principle

A unified dynamical field theory of learning, inference, and emergence is developed in this work. Starting from a minimal stochastic dynamical equation, we showed that inference corresponds to saddle-point trajectories of an MSRJD action, while emergent collective phenomena arise inevitably from fluctuations around these trajectories through loop corrections. This framework provides a single theoretical language connecting energy-based models, recurrent neural networks, transformer architectures, and biologically motivated homeostatic dynamics.

A central conceptual implication of this theory is a reinterpretation of inference as a dynamical process rather than an algorithmic operation. In the present framework, inference is realized as relaxation along stable directions of a learned potential landscape embedded in a nontrivial state-space geometry. Learning does

not compute solutions explicitly; instead, it sculpts the effective potential Φ and the metric G , thereby jointly shaping both the landscape and the geometry on which inference unfolds. This geometric perspective naturally explains the robustness of inference across diverse implementations, from biological neural circuits to artificial architectures, despite substantial microscopic variability and noise.

A key result of our analysis is that emergence is not an optional or fine-tuned feature of cognitive dynamics. Whenever nonlinear interactions and stochastic fluctuations coexist, loop corrections necessarily generate new collective time scales and modes. This mechanism closely parallels the emergence of quasiparticles in condensed matter physics, where collective excitations arise from the self-consistent dressing of microscopic dynamics by fluctuations. In the present context, such emergent collective modes provide a natural substrate for memory, temporal integration, and slow cognitive dynamics that are inaccessible at the level of mean-field or single-unit descriptions.

The unified dynamical theory also offers a coherent explanation for several characteristic features of biological neural systems. Homeostatic regulation stabilizes activity amplitudes and shapes the effective potential, reentrant connectivity generates non-conservative flows that support iterative reinterpretation and contextual modulation, and critical slowing down near soft modes enables extended temporal integration without loss of stability. These features are difficult to reconcile within purely feedforward or static energy-based models, yet arise generically within the present framework as collective dynamical phenomena.

Cognitive field interpretation. The geometric structure underlying the unified dynamical equation naturally admits an interpretation in terms of a *cognitive field*. By this term, we do not posit a new physical field in the electromagnetic or relativistic sense, but refer to an effective dynamical field defined on the collective state space, whose structure jointly governs learning, inference, and emergent cognitive dynamics.

Within this interpretation, the collective state evolves under a state-space vector field whose gradient component, shaped by the effective potential Φ and the metric G , implements inference as relaxation toward dynamically stabilized manifolds, while the non-conservative reentrant component defines an autonomous solenoidal flow that redistributes activity along these manifolds without altering the potential. Crucially, the presence of this reentrant component is not a modeling embellishment but a geometric necessity once a metric structure on state space is specified.

Interpreting the unified dynamics as a cognitive field places learning, inference, and emergence on the same conceptual footing as field-theoretic descriptions in statistical physics, where macroscopic behavior is governed

by effective fields rather than microscopic details. In this sense, the cognitive field provides a compact and principled language for summarizing how learned geometry, reentrant dynamics, and collective time-scale organization jointly support stable yet flexible cognition in high-dimensional, noisy systems.

B. Collective Time Scales and the Time-Scale Density of States

A particularly important outcome of this work is the identification of the *time-scale density of states* as a physically meaningful descriptor of cognition. Neural systems are composed of heterogeneous, irregularly connected, and intrinsically stochastic elements, a fact that has long obscured how stable inference and memory can arise. Within the present framework, this apparent paradox is resolved by recognizing that cognitive function is governed not by microscopic precision, but by the collective organization of dynamical time scales. Learning and homeostatic adaptation reshape the TDOS, selectively stabilizing slow collective modes while suppressing unstable or spurious directions through the joint modulation of potential structure and state-space geometry. Cognition thus corresponds to the controlled persistence of these slow modes, which integrate information over extended time intervals and remain robust against noise and microscopic variability.

From this perspective, different cognitive states or computational regimes are naturally distinguished by their TDOS profiles, reflecting the presence, absence, or reorganization of slow collective modes. This interpretation implies that measurements of temporal correlations, power spectra, or relaxation dynamics can serve as direct probes of cognitive function, without relying on detailed anatomical descriptions or single-neuron precision. Such observables provide a direct and experimentally accessible link between dynamical field-theoretic descriptions and empirical studies of neural systems.

In a broader theoretical context, the TDOS-based description places the present framework in continuity with a class of dynamical models in which functionally relevant structure emerges through temporal correlations rather than spatial order. Oscillatory instabilities captured by the Stuart–Landau (Hopf normal form) and synchronization transitions in the Kuramoto model exemplify low-dimensional cases where criticality manifests as slow collective time scales [43–45]. The present theory extends these paradigmatic examples by offering a unified field-theoretic language for describing how entire spectra of collective time scales are dynamically organized and reshaped by learning, reentrant dynamics, and adaptive state-space geometry in high-dimensional systems. In this sense, TDOS provides a principled and experimentally accessible bridge between canonical models

of temporal criticality and the adaptive dynamics underlying cognition.

C. Implications for Artificial Intelligence and Architecture Design

In the context of artificial intelligence, the present theory suggests that the empirical success of modern architectures does not primarily stem from architectural complexity, but from their implicit approximation of a unified underlying dynamical equation. Residual connections, normalization layers, and attention mechanisms may be interpreted as discrete implementations of continuous recurrent flows constrained by a learned state-space geometry. From this standpoint, principled strategies for architecture design emerge naturally, emphasizing stability, reentry, and geometric regularization rather than ad hoc structural elaboration.

Within this dynamical interpretation, the expressive power of modern transformer architectures admits a clarifying explanation. Their apparent intelligence does not arise solely from the explicit optimization of an objective function, but from the ability to dynamically reshape the effective geometry of representation space in a state-dependent manner. Attention mechanisms implement this adaptive geometric reweighting at the level of computation, while the training objective acts as a background potential that biases selection within the induced geometry. Accordingly, attention does not introduce a fundamentally new mode of computation, but realizes a discrete approximation to inference on a learned, context-dependent state-space geometry.

D. Outlook and Open Questions

Several open questions remain. While the present analysis establishes the inevitability of emergent collective modes, a detailed classification of universality classes for learning dynamics remains to be developed. The precise biological mechanisms implementing effective noise, homeostatic regulation, and metric learning in neural circuits warrant further investigation. In addition, the role of higher-order loop corrections and nonperturbative effects near strong criticality remains an important open problem.

Looking forward, the framework developed here suggests concrete and experimentally accessible routes for testing the proposed dynamical principles of cognition. If inference and cognitive stability are governed by the collective organization of time scales, this structure should be directly reflected in measurable temporal correlations of neural activity. The TDOS may be inferred from empirical autocorrelation functions, power spectra, or linear response measurements in large-scale neural recordings.

Systematic reorganization of the TDOS under learning, adaptation, or task engagement provides a direct and falsifiable prediction of the theory.

More broadly, the present work suggests that learning, inference, and emergence are not disparate phenomena, but manifestations of a single dynamical principle. In this sense, the unified dynamical equation proposed here may serve as a foundational law for understanding collective intelligence in both natural and artificial systems.

VIII. CONCLUSION

We have developed a unified dynamical field-theoretic framework for learning, inference, and emergence, identifying a minimal physical principle underlying cognitive dynamics. Within this framework, inference corresponds to saddle-point trajectories of an MSRJD action, realized as deterministic relaxation flows on a learned, state-dependent geometry of collective state space, while fluctuation-induced loop corrections generically generate collective modes and characteristic time scales beyond mean-field descriptions.

A central result of this work is that cognitive function is governed not by microscopic units or precise activity patterns, but by the collective organization of dynamical time scales across the full joint state space. We introduced the time-scale density of states as a compact and physically meaningful descriptor of this organization, providing a unified diagnostic for inference dynamics across biological and artificial systems. Learning and homeostatic regulation are naturally interpreted as processes that reshape the effective potential and the underlying state-space geometry, thereby reorganizing the TDOS and selectively stabilizing slow collective modes that support robust inference, memory, and context-dependent computation.

By shifting the focus from individual components to collective time-scale structure, and to the geometry that governs sensitivity and stability of inference trajectories, the present theory explains how stable cognition can emerge from heterogeneous, stochastic, and irregular substrates. More broadly, it suggests that learning, inference, and emergence are not distinct processes, but manifestations of a single dynamical principle governing high-dimensional adaptive systems.

Acknowledgements—This work was partially supported by the Institute of Information & Communications Technology Planning & Evaluation (IITP) grant funded by the Korea government (MSIT) (IITP-RS-2025-02214780).

The author acknowledges the support of ChatGPT (GPT-5, OpenAI) for assistance in literature review and conceptual structuring during early development.

-
- [1] G. M. Edelman, *Neural Darwinism: The Theory of Neuronal Group Selection* (Basic Books, New York, 1989).
 - [2] G. Tononi, O. Sporns, and G. M. Edelman, “A measure for brain complexity: Relating functional segregation and integration in the nervous system,” *Proc. Natl. Acad. Sci. USA* **91**, 5033-5037 (1994).
 - [3] D. R. Chialvo, “Emergent complex neural dynamics,” *Nat. Phys.* **6**, 744-750 (2010).
 - [4] W. Gerstner, W. M. Kistler, R. Naud, and L. Paninski, *Neuronal Dynamics* (Cambridge University Press, 2014).
 - [5] G. G. Turrigiano and S. B. Nelson, “Hebb and homeostasis in neuronal plasticity,” *Curr. Opin. Neurobiol.* **10**, 358-364 (2000).
 - [6] L. F. Abbott and W. G. Regehr, “Synaptic computation,” *Nature* **431**, 796-803 (2004).
 - [7] J. M. Beggs and D. Plenz, “Neuronal avalanches in neocortical circuits,” *J. Neurosci.* **23**, 11167-11177 (2003).
 - [8] M. Schuster and K. K. Paliwal, “Bidirectional recurrent neural networks,” *IEEE Trans. Signal Process.* **45**, 2673-2681 (1997).
 - [9] A. Vaswani, N. Shazeer, N. Parmar, J. Uszkoreit, L. Jones, A. N. Gomez, L. Kaiser, and I. Polosukhin, “Attention is all you need,” arXiv:1706.03762 (2017).
 - [10] J. Wei, Y. Tay, R. Bommasani, C. Raffel, B. Zoph, S. Borgeaud, D. Yogatama, M. Bosma, D. Zhou, D. Metzler, E. H. Chi, T. Hashimoto, O. Vinyals, P. Liang, J. Dean, and W. Fedus, “Emergent abilities of large language models,” *Transactions on Machine Learning Research* (2022).
 - [11] S. Yao, J. Zhao, D. Yu, N. Du, I. Shafraan, K. Narasimhan, and Y. Cao, “ReAct: Synergizing reasoning and acting in language models,” arXiv:2210.03629 (2022).
 - [12] J. J. Hopfield, “Neural networks and physical systems with emergent collective computational abilities,” *Proc. Natl. Acad. Sci. USA* **79**, 2554-2558 (1982).
 - [13] D. J. Amit and H. Gutfreund, “Storing infinite numbers of patterns in a spin-glass model of neural networks,” *Phys. Rev. Lett.* **55**, 1530-1533 (1985).
 - [14] P. Cannon and J. Miller, “Synaptic and intrinsic homeostasis cooperate to optimize single neuron response properties and tune integrator circuits,” *J. Neurophysiol.* **116**, 2004-2022 (2016).
 - [15] N. Niemeyer, J. H. Schleimer, and S. Schreiber, “Biophysical models of intrinsic homeostasis: Firing rates and beyond,” *Curr. Opin. Neurobiol.* **70**, 81-88 (2021).
 - [16] G. E. Hinton and D. C. Plaut, “Using fast weights to deblur old memories,” *Proc. 9th Annu. Conf. Cognitive Science Society*, 177-186 (1987).
 - [17] J. Schmidhuber, “Learning to control fast-weight memories: An alternative to dynamic recurrent networks,” *Neural Comput.* **4**, 131-139 (1992).
 - [18] I. Schlag, T. Irie, and J. Schmidhuber, “Linear transformers are secretly fast weight programmers,” arXiv:2102.11174 (2021).
 - [19] A. Katharopoulos, A. Vyas, N. Pappas, and F. Fleuret, “Transformers are RNNs: Fast autoregressive transformers with linear attention,” arXiv:2006.16236 (2020).
 - [20] K. G. Wilson and J. Kogut, “The renormalization group and the ϵ expansion,” *Phys. Rep.* **12**, 75-199 (1974).
 - [21] J. Cardy, *Scaling and Renormalization in Statistical Physics* (Cambridge University Press, Cambridge, 1996).

- [22] U. C. Täuber, *Critical Dynamics* (Cambridge University Press, Cambridge, 2014).
- [23] J. Zinn-Justin, *Quantum Field Theory and Critical Phenomena* (Oxford University Press, Oxford, 2002).
- [24] P. C. Martin, E. D. Siggia, and H. A. Rose, “Statistical dynamics of classical systems,” *Phys. Rev. A* **8**, 423-437 (1973).
- [25] H. K. Janssen, “On a Lagrangian for classical field dynamics and renormalization group calculations of dynamical critical properties,” *Z Phys B* **23**, 377-380 (1976).
- [26] C. De Dominicis, “Techniques de renormalisation de la théorie des champs et dynamique des phénomènes critiques,” *J. Phys. Colloq.* **37**, 247-253 (1976).
- [27] J. M. Horowitz and M. Esposito, “Thermodynamics with continuous information flow,” *Phys. Rev. X* **4**, 031015 (2014).
- [28] P. Bak, C. Tang, and K. Wiesenfeld, “Self-organized criticality: An explanation of $1/f$ noise,” *Phys. Rev. Lett.* **59**, 381-384 (1987).
- [29] B. G. Chae, “Self-organized criticality from protected mean-field dynamics: Loop stability and internal renormalization in reflective neural systems,” arXiv:2601.04450 (2026).
- [30] P. Bak, *How Nature Works: The Science of Self-Organized Criticality* (Springer, New York, 1996).
- [31] H. J. Jensen, *Self-Organized Criticality: Emergent Complex Behavior in Physical and Biological Systems* (Cambridge University Press, Cambridge, 1998).
- [32] R. Dickman, M. A. Muñoz, A. Vespignani, and S. Zapperi, “Paths to self-organized criticality,” *Braz. J. Phys.* **30**, 27-41 (2000).
- [33] S. Bornholdt and T. Rohlf, “Topological evolution of dynamical networks: Global criticality from local dynamics,” *Phys. Rev. Lett.* **84**, 6114-6116 (2000).
- [34] A. Levina, J. M. Herrmann, and T. Geisel, “Phase transitions towards criticality in a neural system with adaptive interactions,” *Phys. Rev. Lett.* **102**, 118110 (2009).
- [35] K. Funahashi and Y. Nakamura, “Approximation of dynamical systems by continuous time recurrent neural networks,” *Neural Networks* **6**, 801-806 (1993).
- [36] R. D. Beer, “On the dynamics of small continuous-time recurrent neural networks,” *Adaptive Behavior* **3**, 469-509 (1995).
- [37] R. Hasani, M. Lechner, A. Amini, D. Rus, and R. Grosu, “Liquid time-constant networks,” *Proc. AAAI Conf. Artif. Intell.* **35**, 7657-7666 (2021).
- [38] B. G. Chae, “Recursive dynamics in fast-weights homeostatic reentry networks: Toward reflective intelligence,” arXiv:2511.06798 (2025).
- [39] B. G. Chae, “Continuous-time homeostatic dynamics for reentrant inference models,” arXiv:2512.05158 (2025).
- [40] B. G. Chae, “Renormalization-group geometry of homeostatically regulated reentry networks,” arXiv:2512.19086 (2025).
- [41] F. W. Warner, *Foundations of Differentiable Manifolds and Lie Groups* (Springer-Verlag, Berlin, 1983).
- [42] S. I. Amari, “Differential geometry of curved exponential families-curvatures and information loss,” *Ann. Statist.* **10**, 357-385 (1982).
- [43] J. T. Stuart, “On the non-linear mechanics of hydrodynamic stability,” *J. Fluid Mech.* **4**, 1-21 (1958).
- [44] O. Kogan, J. L. Rogers, M. C. Cross, and G. Refael, “Renormalization group approach to oscillator synchronization,” *Phys. Rev. E* **80**, 036206 (2009).
- [45] J. A. Acebrón, L. L. Bonilla, C. J. Pérez Vicente, F. Ritort, and R. Spigler, “The Kuramoto model: A simple paradigm for synchronization phenomena,” *Rev. Mod. Phys.* **77**, 137-185 (2005).

Supplementary Materials

Appendix A: Computation and Inference of the Time-Scale Density of States

This provides technical details on how the time-scale density of states (TDOS) introduced in Sec. IV can be computed from models and simulations, as well as inferred from observed activity. These results establish that the TDOS is not merely a conceptual construct, but a quantitatively well-defined and experimentally accessible object.

(I) *Computation from models and simulations:* Consider the unified dynamical equation

$$\dot{x} = -G^{-1}(x)\nabla\Phi(x) + R(x) + \xi(t), \quad (\text{S1})$$

and let $x^*(t)$ denote a representative fixed point or inference trajectory. Linearizing the deterministic drift around $x^*(t)$ yields

$$\delta\dot{x} = -M\delta x + \eta, \quad (\text{S2})$$

where the linear stability matrix M is given by

$$M = -\frac{\partial}{\partial x} (-G^{-1}\nabla\Phi + R) \Big|_{x^*(t)}. \quad (\text{S3})$$

For time-independent fixed points, M is constant in time, whereas for slowly varying inference trajectories one may consider a quasi-static approximation.

Let $\{\mu_\alpha\}$ denote the eigenvalues of M . Because reentrant dynamics generally renders M non-symmetric, the relevant relaxation rates are given by the real parts of the spectrum,

$$\lambda_\alpha \equiv \text{Re}(\mu_\alpha). \quad (\text{S4})$$

The normalized TDOS is then defined as

$$\rho(\lambda) = \frac{1}{N} \sum_{\alpha=1}^N \delta(\lambda - \lambda_\alpha). \quad (\text{S5})$$

In numerical practice, the delta functions are replaced by a smooth kernel,

$$\rho_\epsilon(\lambda) = \frac{1}{N} \sum_{\alpha} \frac{1}{\sqrt{2\pi\epsilon}} \exp\left[-\frac{(\lambda - \lambda_\alpha)^2}{2\epsilon^2}\right], \quad (\text{S6})$$

which provides a stable estimate of the TDOS and allows direct visualization of the distribution of collective

time scales. Importantly, physically relevant behavior is controlled not by an individual eigenvalue, but by the accumulation of spectral weight in $\rho(\lambda)$ near slow relaxation rates.

(II) *Inference of the TDOS from observed activity:* The TDOS can also be inferred directly from observed activity without explicit knowledge of microscopic model parameters. Within the stationary Ornstein–Uhlenbeck approximation, fluctuations around an inference trajectory satisfy

$$\delta\dot{x} = -M\delta x + \eta, \quad (\text{S7})$$

with corresponding retarded response function

$$G_R(\omega) = (-i\omega + M)^{-1}. \quad (\text{S8})$$

The correlation function is given by

$$C(\omega) = 2D G_R(\omega) G_R^\dagger(\omega). \quad (\text{S9})$$

When M is symmetric, or approximately so, the trace of the correlation function admits the spectral representation

$$\text{Tr} C(\omega) \propto \sum_{\alpha} \frac{1}{\omega^2 + \lambda_\alpha^2} = \int d\lambda \rho(\lambda) \frac{1}{\omega^2 + \lambda^2}. \quad (\text{S10})$$

Thus, the observed power spectrum is an integral transform of the TDOS with a Lorentzian kernel. In practice, one may average power spectra across channels and invert Eq. (S10) using appropriate regularization to obtain a robust estimate of $\rho(\lambda)$ from data. This establishes a direct connection between experimentally measured temporal correlations and the collective time-scale structure of the dynamics.

(III) *Resolvent representation and large- N limit:* In the large- N limit, the TDOS becomes a smooth function and admits a compact representation in terms of the resolvent,

$$G_z(z) = \frac{1}{N} \text{Tr} (zI - M)^{-1}. \quad (\text{S11})$$

The TDOS is then obtained as

$$\rho(\lambda) = \frac{1}{\pi} \lim_{\epsilon \rightarrow 0^+} \text{Im} G_z(\lambda + i\epsilon). \quad (\text{S12})$$

This expression is mathematically identical to the Green's function representation of the density of states in condensed matter physics, with the stability matrix M playing the role of an effective dynamical operator.

For disordered or high-dimensional systems, the spectrum of M generically forms a continuous band rather than isolated eigenvalues, reflecting the presence of many overlapping collective modes. The TDOS therefore provides a natural and physically meaningful description of collective dynamics in large recurrent systems.

(IV) *Effect of loop corrections*: Loop corrections renormalize the effective stability matrix according to

$$M_{\text{eff}}(\omega) = M - \Sigma_R(\omega), \quad (\text{S13})$$

and, in particular, modify the low-frequency spectrum through $M_{\text{eff}} \simeq M - \Sigma_R(0)$. As a consequence, the TDOS itself is renormalized,

$$\rho(\lambda) \rightarrow \rho_{\text{eff}}(\lambda), \quad (\text{S14})$$

providing a precise sense in which fluctuations reorganize the distribution of collective time scales. This renormalization underlies the emergence of slow collective modes and dynamically generated infrared cutoffs discussed in Sec. IV.

Although a finite system possesses only N discrete relaxation rates, for large N the physically relevant quantity is the density of modes near a given time scale. Learning and adaptation may therefore be interpreted as processes that reshape the TDOS, selectively enhancing or suppressing collective modes that govern inference and memory.

Appendix B: Derivation of the FHRN Decomposition

We provide a detailed derivation of the decomposition of the FHRN dynamics into a radial gradient flow generated by an effective potential, an anisotropic, state-dependent metric, and a non-conservative reentrant flow tangent to the stabilized manifold.

(I) *Full FHRN dynamics and exact radial reduction*: We begin with the continuous-time FHRN equation,

$$\dot{y} = -y + \gamma W[g(r)y], \quad r = \|y\|, \quad (\text{S15})$$

where $y \in \mathbb{R}^N$ denotes collective population activity, W is a fixed linear mixing operator, γ controls reentry strength, and $g(r)$ is a scalar homeostatic gain depending only on the global amplitude r .

We assume that W admits a dominant eigenvalue ρ with associated eigenvector v_0 , and that the remaining spectrum is bounded away from ρ .

Taking the time derivative of $r = \|y\|$ yields

$$\dot{r} = \frac{y \cdot \dot{y}}{r}. \quad (\text{S16})$$

Substituting Eq. (S15) gives

$$\dot{r} = -r + \gamma g(r) \frac{y^\top W y}{r}. \quad (\text{S17})$$

Projecting y onto the dominant eigenspace of W and assuming alignment with the leading eigenvector, $y \approx r v_0$, one obtains

$$y^\top W y \approx \rho r^2. \quad (\text{S18})$$

Under this dominant-eigenmode approximation, the radial dynamics closes as

$$\dot{r} = [-1 + \gamma \rho g(r)] r. \quad (\text{S19})$$

(II) *Effective radial potential*: Equation (S19) can be written in gradient form,

$$\dot{r} = -\frac{d\Phi(r)}{dr}, \quad (\text{S20})$$

with

$$\frac{d\Phi}{dr} = [1 - \gamma \rho g(r)] r. \quad (\text{S21})$$

For the homeostatic gain

$$g(r) = \frac{1}{1 + \kappa(r^2 - 1)}, \quad (\text{S22})$$

direct integration yields the effective potential

$$\Phi(r) = \frac{1}{2} r^2 - \frac{\gamma \rho}{2\kappa} \ln[1 + \kappa(r^2 - 1)] + \text{const.} \quad (\text{S23})$$

This potential develops a stable minimum at finite r for $\gamma \rho > 1$, corresponding to a homeostatically stabilized activity shell.

(III) *Projector decomposition and emergent metric*: To analyze fluctuations around the shell, we introduce the radial and tangential projectors,

$$P_r = \frac{y y^\top}{r^2}, \quad P_\perp = I - P_r. \quad (\text{S24})$$

Decomposing the drift in Eq. (S15) yields

$$\dot{y} = -P_r y - P_\perp y + \gamma g(r) (P_r W y + P_\perp W y). \quad (\text{S25})$$

The radial component reproduces the gradient flow generated by $\Phi(r)$, while the tangential component remains unconstrained by the potential.

This separation implies an effective anisotropic metric of the form

$$G(y) = g_r(r) P_r + g_\perp(r) P_\perp, \quad (\text{S26})$$

with $g_r(r) \gg g_\perp(r)$ near the stabilized shell. Importantly, this metric is not externally imposed but emerges from the homeostatic suppression of radial fluctuations.

(IV) *Reentrant tangential flow*: The remaining tangential dynamics defines a non-conservative reentrant flow,

$$R(y) = \gamma g(r) P_\perp W y, \quad (\text{S27})$$

which satisfies

$$y \cdot R(y) = 0. \quad (\text{S28})$$

Hence $R(y)$ redistributes activity along the shell without affecting the stabilized amplitude r .

Because R cannot be expressed as the gradient of any scalar potential, it represents a genuine reentrant contribution, inducing rotational and mixing dynamics on the low-dimensional attractor manifold.

(V) *Relation to the unified dynamical equation:* Collecting the above results, the FHRN dynamics can be written in the unified form

$$\dot{y} = -G^{-1}(y) \nabla_y \Phi(y) + R(y), \quad (\text{S29})$$

where Φ controls radial stability, G encodes the dynamically generated state-space geometry, and R implements non-conservative reentry.

This decomposition clarifies the conceptual distinction between the FHRN and standard recurrent or transformer architectures: both the effective potential and the geometry of state space emerge from the dynamics itself, rather than being imposed externally.

Appendix C: Emergent Riemannian Geometry from Homeostatic Shell Dynamics

Homeostatic regulation strongly suppresses radial excursions of collective activity while leaving tangential degrees of freedom comparatively unconstrained. As a result, the effective continuous-time dynamics near the stabilized shell is most naturally expressed in terms of an anisotropic, state-dependent metric of the form Eq. (S26). Importantly, this metric is not imposed externally. Rather, it provides a compact representation of the differential sensitivity of the underlying probabilistic inference dynamics, and may be interpreted as an effective Fisher information metric induced by homeostatic shell dynamics and pulled back to the collective state space.

(I) *Non-Euclidean nature of the induced geometry:* A crucial consequence of this construction is that the metric $G(y)$ is not spatially constant and therefore does not correspond to a Euclidean geometry. Since both the radial and tangential projectors, $P_r(y)$ and $P_\perp(y)$, depend explicitly on the state vector y , their derivatives are generically nonzero, implying

$$\partial_k G_{ij}(y) \neq 0 \quad (\text{S30})$$

throughout the neighborhood of the homeostatic shell.

Consequently, the associated Levi-Civita connection,

$$\Gamma^i_{jk} = \frac{1}{2} G^{i\ell} (\partial_j G_{k\ell} + \partial_k G_{j\ell} - \partial_\ell G_{jk}), \quad (\text{S31})$$

does not vanish even arbitrarily close to the stabilized manifold. This immediately implies a nontrivial Riemann curvature tensor,

$$R^i_{jkl}[G] = \partial_k \Gamma^i_{jl} - \partial_l \Gamma^i_{jk} + \Gamma^i_{km} \Gamma^m_{jl} - \Gamma^i_{lm} \Gamma^m_{jk}, \quad (\text{S32})$$

which is generically nonzero.

Thus, the shell formed by homeostatic regulation is not merely a constrained subset of an ambient Euclidean space. Instead, it induces a genuinely non-Euclidean state-space geometry endowed with intrinsic Riemann curvature, reflecting the state-dependent sensitivity of probabilistic inference.

(II) *Geodesic deviation and cognitive tidal forces:* The dynamical implications of this curvature become explicit through the geodesic deviation equation. Let $\zeta^i(t)$ denote the separation vector between two nearby inference trajectories evolving under identical dynamics. Its evolution obeys

$$\frac{D^2 \zeta^i}{Dt^2} = -R^i_{jkl}[G] \dot{y}^j \zeta^k \dot{y}^l, \quad (\text{S33})$$

where D/Dt denotes the covariant time derivative along the trajectory.

Depending on the local sectional curvature of the state space, nearby trajectories may undergo focusing or defocusing. Positive curvature leads to convergence of trajectories, while negative curvature induces divergence and branching. Crucially, these effects arise independently of the Hessian of the potential Φ , stochastic fluctuations, or instabilities of initial conditions. They represent a purely geometric mechanism originating from the curvature of the state-space metric.

In the continuous-time limit of the FHRN dynamics, homeostatic regulation stabilizes activity on a finite-radius shell, enforcing a pronounced radial-tangential anisotropy in the effective dynamics. This anisotropy is naturally encoded in the induced state-dependent metric and inevitably gives rise to a non-Euclidean Riemannian geometry.

We interpret the resulting curvature-induced relative acceleration between nearby inference trajectories as *cognitive tidal forces*: a geometric manifestation of the information-theoretic sensitivity encoded in the Fisher metric, regulating inference sensitivity, trajectory branching, and the selection of slow collective modes beyond what can be captured by potential structure alone.

Appendix D: A minimal Fisher-information derivation of the shell metric

Here we show, in a concrete and minimal probabilistic setting, how a Fisher-information metric on the collective state space naturally acquires the same radial-tangential projector structure as the FHRN metric, $G(y) = g_r(r)P_r + g_\perp(r)P_\perp$. The purpose is not to claim a unique generative model, but to exhibit a simple class of distributions whose local information geometry *necessarily* takes this form whenever radial and tangential sensitivities are separated.

(I) *Anisotropic Gaussian family on \mathbb{R}^N* : Let $x \in \mathbb{R}^N$ denote the latent collective state and $z \in \mathbb{R}^N$ an “internal observation” (or self-generated prediction target) drawn from a Gaussian likelihood centered at x ,

$$p(z|x) = \mathcal{N}(z; x, \Sigma(x)), \quad (\text{S34})$$

with an anisotropic covariance aligned with radial and tangential subspaces at the current state:

$$\begin{aligned} \Sigma(x) &= \sigma_r^2(r) P_r(x) + \sigma_\perp^2(r) P_\perp(x), & r &= \|x\|, \\ P_r &= \frac{xx^\top}{r^2}, & P_\perp &= I - P_r. \end{aligned} \quad (\text{S35})$$

This is the simplest rotationally covariant way to encode the idea that radial fluctuations are more strongly suppressed than tangential ones near a stabilized shell (e.g., $\sigma_r(r) \ll \sigma_\perp(r)$ for $r \approx r_*$).

Since P_r and P_\perp are orthogonal projectors, the inverse covariance has the same projector form,

$$\Sigma^{-1}(x) = \frac{1}{\sigma_r^2(r)} P_r(x) + \frac{1}{\sigma_\perp^2(r)} P_\perp(x). \quad (\text{S36})$$

(II) *Fisher information for the mean parameter*: For a Gaussian with mean x and (locally) fixed covariance, the score function is

$$\partial_i \log p(z|x) = [\Sigma^{-1}(x)(z-x)]_i \quad (\text{neglecting } \partial_i \Sigma \text{ terms}). \quad (\text{S37})$$

This approximation is appropriate when the dominant sensitivity arises from mean shifts (the “prediction error” $z-x$) and the variation of Σ with x is subleading on the scale of typical fluctuations. Under this standard simplification,

$$F_{ij}(x) \equiv \mathbb{E}_{z|x} \left[\partial_i \log p(z|x) \partial_j \log p(z|x) \right] = [\Sigma^{-1}(x)]_{ij}, \quad (\text{S38})$$

because $\mathbb{E}_{z|x} [(z-x)(z-x)^\top] = \Sigma(x)$.

Combining Eqs. (S36)–(S38) yields the Fisher metric in projector form:

$$\begin{aligned} F(x) &= f_r(r) P_r(x) + f_\perp(r) P_\perp(x), & f_r(r) &= \sigma_r^{-2}(r), \\ f_\perp(r) &= \sigma_\perp^{-2}(r). \end{aligned} \quad (\text{S39})$$

Thus, whenever radial and tangential uncertainties differ, the induced information geometry is *spherically symmetric but anisotropic*: it preserves rotational covariance while assigning distinct local length scales to radial and tangential directions.

(III) *Identification with the FHRN shell metric*: Equation (S39) matches the metric structure used in the FHRN decomposition upon the identification

$$\begin{aligned} G(x) &\propto F(x), & g_r(r) &\propto f_r(r) = \sigma_r^{-2}(r), \\ g_\perp(r) &\propto f_\perp(r) = \sigma_\perp^{-2}(r). \end{aligned} \quad (\text{S40})$$

In particular, homeostatic stabilization of the shell corresponds to $\sigma_r(r_*) \ll \sigma_\perp(r_*)$ and therefore to a strongly anisotropic Fisher geometry with $g_r(r_*) \gg g_\perp(r_*)$, capturing the empirical fact that radial excursions are tightly constrained while tangential degrees of freedom remain comparatively free.

If one retains the full x -dependence of $\Sigma(x)$, additional terms from $\partial_i \Sigma$ enter the score and Fisher information. However, for rotationally covariant families of the form Eq. (S35), these corrections preserve the same radial–tangential decomposition and merely renormalize the scalar coefficients $f_r(r), f_\perp(r)$. Therefore the projector structure is robust: it follows from symmetry and the separation of radial and tangential sensitivities, not from the Gaussian choice itself.